

Numerical Analysis of Convection in the Inner Core (DRAFT)

Maximilian Williams

September 2021

Abstract

Convection in the Earth's inner core has been a contentious topic in geoscience. Recently, it has been proposed through seismic observations that Earth's inner core is convecting. Here we numerically model the Earth's inner core as a self-gravitating internally heated fluid bousinesque fluid in 2-dimensions using a streamfunction-vorticity method and Thermal Lattice Boltzman approach. The streamfunction-vorticity approach is studied using two codes in cartesian and polar coordinates. The streamfunction and Thermal Lattice Boltzman codes are written from scratch in python3 and goLang.

Introduction

Governing Equations

In this section I introduce the physics of the problem; the governing equations that we wish to numerically solve.

Throughout analysis we describe the fluid in the Eulerian frame under a gravitational acceleration \vec{g} which may vary in space. We give each location in the fluid a velocity \vec{u} and density ρ that vary in space \vec{x} and time t . We assume the fluid's viscosity μ and thermal diffusivity κ are constant. By conserving fluid momentum, we produce the Navier-Stokes equation:

$$\rho \frac{D\vec{u}}{Dt} = \rho \vec{g} - \nabla p + \mu \nabla^2 \vec{u}, \quad (1)$$

where $\frac{D}{Dt} = \frac{\partial}{\partial t} + (\vec{u} \cdot \nabla)$ is the material derivative, p the pressure of the fluid and ∇ the del operator. The dynamics of fluid temperature T are described by the inhomogeneous advection-diffusion equation:

$$\frac{DT}{Dt} = \kappa \nabla^2 T + H, \quad (2)$$

where H is internal heating. The density of the fluid ρ is assumed to vary linearly in temperature according to the equation of state:

$$\rho = \rho_0(1 - \alpha(T - T_0)), \quad (3)$$

where α is the volumetric expansion coefficient and ρ_0 the density at a reference temperature T_0 . Through seismic imaging, variations in inner core density are $\ll 1\%$ (check this claim). We also assume that the inner core's evolution occurs over geologic timescales, and as such take \vec{u} to be first order. These assumptions allow us to make the slow flow Boussinesq approximation to equation 1:

$$\frac{\partial \vec{u}}{\partial t} = \frac{\rho'}{\rho} \vec{g} - \frac{\nabla p'}{\rho_0} + \nu \nabla^2 \vec{u}, \quad (4)$$

where $\rho' = -\alpha(T - T_0)$, ν the kinematic viscosity $\nu = \frac{\mu}{\rho_0}$ and p' a first order perturbation to the background pressure p_0 . We use two numbers to characterise the convection in the problem, the Prandtl number and the Rayleigh number. The Rayleigh number characterises

$$Pr = \frac{\nu}{\kappa} \quad (5)$$

Numerical Methods

Two numerical methods are introduced for solving the thermal convection problem, the Lattice Boltzman Method and the streamfunction-vorticity formulation.

Streamfunction-Vorticity formulation

Here I introduce the streamfunction-vorticity method for use in 2 dimensions and use it to eliminate pressure terms in 4 and 2 in cartesian and polar geometries giving a set of numerically solvable equations.

The streamfunction-vorticity formulation is a popular method for analytical and simple numerical analysis of incompressible fluids in two dimensions. Its main advantage is its elimination of all pressure terms, which would typically require iterative techniques to

solve, as is used in the SIMPLE algorithm. However, the streamfunction-vorticity method is limited to 2-dimensional or 3-dimensional symmetric flows and so has limited applicability.

We define two scalar quantities, the vorticity ω and the streamfunction ψ . The vorticity ω is given by:

$$\omega = (\nabla \times \vec{u})_z, \quad (6)$$

where the z subscript denotes the component out of the plane. We also define a streamfunction ψ by:

$$\omega = -\nabla^2 \psi. \quad (7)$$

Given a coordinate system, and a clever definition of \vec{u} we can rewrite equations 2 and 4 in terms of ω and ψ rather than \vec{u} and p . In cartesian coordinates (x, y) we pick

$$u = \frac{\partial \psi}{\partial y}, v = -\frac{\partial \psi}{\partial x}, \quad (8)$$

allowing us to write equations 2 and 4 as:

$$\frac{\partial T}{\partial t} + \frac{\partial \psi}{\partial y} \frac{\partial T}{\partial x} - \frac{\partial \psi}{\partial x} \frac{\partial T}{\partial y} = \kappa \nabla^2 T + \frac{Q}{\rho_0 C_v} \quad (9) \quad \frac{\partial \omega}{\partial t} = -\frac{g_y}{\rho_0} \frac{\partial \rho'}{\partial x} + \nu \nabla^2 \omega \quad (10)$$

Similarly, in polar coordinates (r, θ) we pick:

$$u = \frac{1}{r} \frac{\partial \psi}{\partial \theta}, v = -\frac{\partial \psi}{\partial r}, \quad (11)$$

giving:

$$\frac{\partial T}{\partial t} + \frac{1}{r} \frac{\partial \psi}{\partial \theta} \frac{\partial T}{\partial r} - \frac{1}{r} \frac{\partial \psi}{\partial r} \frac{\partial T}{\partial \theta} = \kappa \nabla^2 T + \frac{Q}{\rho_0 C_v} \quad (12) \quad \frac{\partial \omega}{\partial t} = -\frac{g_r}{\rho_0 r} \frac{\partial \rho'}{\partial \theta} + \nu \nabla^2 \omega. \quad (13)$$

A full derivation of equations 9, 10, 12, 13 are given in appendix. Importantly, our definitions of u and v in equations 8 and 11 satisfy equation 6 and 7. Equations 7, 9, 10 for the cartesian case and 7, 12, 13 for the polar case can be directly solved.

Solving the streamfunction-vorticity equations

The finite difference method used for solving the streamfunction-vorticity-formulated governing equations is shown

We first discretize our domain \mathcal{D} . In the cartesian case, we use $(x_i, y_j) = (i\Delta x, j\Delta y)$ with integers i and j satisfying $0 \leq i < N_x$ $0 \leq j < N_y$. In the polar case, we use $(r_i, \theta_j) = (R_0 + i\Delta r, j\Delta \theta)$ again with $0 \leq i < N_r$ and $0 \leq j < N_\theta$. We impose $\Delta \theta = \frac{2\pi}{N_\theta - 1}$ for consistency with θ -periodic boundary conditions and an inner radius R_0 in polar coordinates to avoid singularities generated by $r = 0$. We also discretize time t by $t_n = n\Delta t$. For a function f , we use $f_{i,j}^n$ to mean f evaluated at time n at position (x_i, y_j) in cartesian coordinates or (r_i, θ_j) in polar coordinates.

To approximate derivatives we use a finite difference approach. All time derivatives are approximated by forward difference:

$$\frac{\partial f}{\partial t} = \frac{f^{n+1} - f^n}{\Delta t} \quad (14)$$

Second order space derivatives are approximated by a central difference:

$$\frac{\partial^2 f_{i,j}}{\partial x_1^2} = \frac{f_{i+1,j} - 2f_{i,j} + f_{i-1,j}}{\Delta x_1^2}, \quad (15) \quad \frac{\partial^2 f_{i,j}}{\partial x_2^2} = \frac{f_{i,j+1} - 2f_{i,j} + f_{i,j-1}}{\Delta x_2^2}, \quad (16)$$

where x_1 is the first coordinate and x_2 is the second coordinate. For example, in cartesian coordinates (x, y) , we would have $x_1 = x$ and $x_2 = y$. For non advection terms, we approximate first order spatial derivatives by:

$$\frac{\partial f_{i,j}}{\partial x_1} = \frac{f_{i+1,j} - f_{i-1,j}}{2\Delta x_1}, \quad (17)$$

and

$$\frac{\partial f_{i,j}}{\partial x_2} = \frac{f_{i,j+1} - f_{i,j-1}}{2\Delta x_2}. \quad (18)$$

For advection terms, of the form $a \frac{\partial f_{i,j}}{\partial x_1}$ we employ a first order godanov scheme:

$$a \frac{\partial f_{i,j}}{\partial x_1} = \frac{1}{\Delta x} (|a| (\frac{1}{2} f_{i+1,j} - \frac{1}{2} f_{i-1,j}) - a (\frac{1}{2} f_{i+1,j} - f_{i,j} - \frac{1}{2} f_{i-1,j})). \quad (19)$$

This scheme is always upstream, regardless of the direction of the advecting field a .

Other more accurate, but substantially more complex methods for solving these equations, particularly the advection equation exists such as the semi-lagrange crank-nicolson scheme.

To solve the streamfunction-vorticity equations we assume a starting vorticity ω on our domain \mathcal{D} . We then apply the Jacobi method to solve equation 7 for ψ on the interior of the domain which we call \mathcal{D}' . Using ψ we update T on \mathcal{D}' using equation 9 (or 12 for polar). Finally, ω is updated on \mathcal{D}' using equation 10 (13 for polar). This process is repeated.

The Jacobi Method

Here a basic numerical method for solving the Poisson equation, the Jacobi method is outlined. We cannot solve for ψ explicitly in equation 7. Instead we use an iterative jacobi method. In cartesian coordinates, equation 7 is:

$$\omega_{i,j} = \frac{\psi_{i+1,j} - 2\psi_{i,j} + \psi_{i-1,j}}{\Delta x^2} + \frac{\psi_{i,j+1} - 2\psi_{i,j} + \psi_{i,j-1}}{\Delta y^2} \quad (20)$$

Rearranging for ψ

$$\psi_{i,j} = \frac{\Delta x^2 \Delta y^2}{2(\Delta x^2 + \Delta y^2)} \left(\frac{\psi_{i+1,j} + \psi_{i-1,j}}{\Delta x^2} + \frac{\psi_{i,j+1} + \psi_{i,j-1}}{\Delta y^2} + \omega_{i,j} \right). \quad (21)$$

We then use the result of $\psi_{i,j}$ back into equation 21 to solve for $\psi_{i,j}$ iterately as shown in equation 22:

$$\psi_{i,j}^{(k+1)} = \frac{\Delta x^2 \Delta y^2}{2(\Delta x^2 + \Delta y^2)} \left(\frac{\psi_{i+1,j}^{(k)} + \psi_{i-1,j}^{(k)}}{\Delta x^2} + \frac{\psi_{i,j+1}^{(k)} + \psi_{i,j-1}^{(k)}}{\Delta y^2} + \omega_{i,j} \right). \quad (22)$$

Where the superscript (k) means the result of the k^{th} iteration of the above equation and this operation us applied to all points in \mathcal{D}' . We terminate this iterative method once the error $\sum_{(i,j) \in \mathcal{D}'} |\psi_{i,j}^{(k+1)} - \psi_{i,j}^{(k)}|$ gets suffeciently small. A similar method is applied to the polar coordinate case.

Lattice Boltzman Method

In this section I give a brief introduction to the Lattice Boltzman Method and why its different from most numerical tehcniques. I introduce a 2-dimensional lattice D2Q9 and discribe the Thermal Lattice Boltzman method (TLBM) which is employed by my numerical solution to simulate convection.

The Lattice Boltzman Method (LBM) is a generalization of a Lattice Gas Automata (LGA), which are themselves a specialized Automata for simulating fluid flows. These Automata methods like common fluid simulation techniques discritize space and time. They directly simulate the state of particles or their distributions and evolve in time accoring to rules which give the desired macroscopic fluid properties as an emergent effect. This is fundamentally different from typical approaches which amount to directly numerically solving a set of partial differential equations.

To discritize space, we place nodes at locations $(x_i, y_j) = (i, j)$ with i, j integers. Each node has attached to it a latitce, here the D2Q9 lattice shown in figure 1. The lattice defines unit vectors \vec{e}_i , $i \in \{0, 1, 2, 3, 4, 5, 6, 7, 8\}$. In addition, each direction e_i gets a weight w_i . In the D2Q9 lattice these are:

$$w_i = \begin{cases} \frac{4}{9} & \text{if } i = 0 \\ \frac{1}{9} & \text{if } i = 1, 2, 3, 4 \\ \frac{1}{36} & \text{if } i = 5, 6, 7, 8 \end{cases}$$

We wish to simulate convection. For this, we require the particle motion and the internal energy throughout the lattice. We define

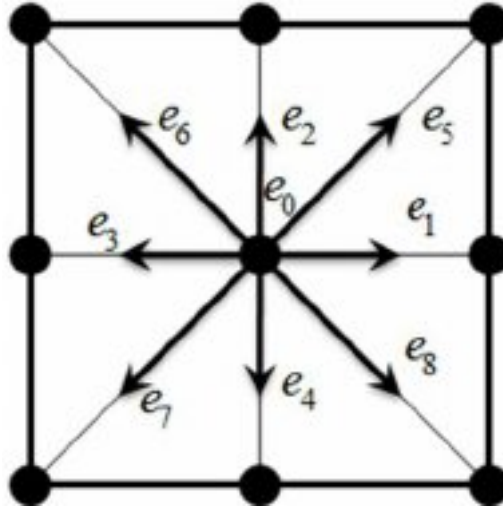


Figure 1: D2Q9 Lattice. Black notes represent lattice points, vectors e_0, \dots, e_8 are the lattice vectors. Image sourced from [2]

two distribution functions $f_\alpha(\vec{x}, t)$ and $g_\alpha(\vec{x}, t)$ denoting the particle and internal energy distributions along direction α at lattice points \vec{x} and times t . The direction can be thought of as the direction of flow for particles or energy. Each timestep there are two steps to updating f and g , a common streaming step:

$$f_\alpha(\vec{x} + \vec{e}_\alpha, t + \Delta t) = f_\alpha(\vec{x}, t), \quad (23)$$

and different collision steps:

$$f_\alpha(\vec{x} + \vec{e}_\alpha, t + \Delta t) = f_\alpha(\vec{x}, t) + \frac{1}{\tau_f}(f_\alpha^{eq}(\vec{x}, t) - f_\alpha(\vec{x}, t)) + F_\alpha \quad (24)$$

$$g_\alpha(\vec{x} + \vec{e}_\alpha, t + \Delta t) = g_\alpha(\vec{x}, t) + \frac{1}{\tau_g}(g_\alpha^{eq}(\vec{x}, t) - g_\alpha(\vec{x}, t)) + G_\alpha. \quad (25)$$

Here F_α and G_α are the forcing terms and f_α^{eq} and g_α^{eq} are equilibrium distributions. The relaxation times τ_f and τ_g are related to the macroscopic thermal diffusivity (κ) and kinematic viscosity ν by:

$$\tau_g = \frac{3\kappa}{S^2\Delta t} + \frac{1}{2}, \quad (26) \quad \tau_f = \frac{3\nu}{S^2\Delta t} + \frac{1}{2}. \quad (27)$$

The equilibrium distributions are given by the BKG approximation:

$$f_\alpha^{eq}(\vec{x}, t) = \rho w_\alpha \left(1 + 3 \frac{\vec{e}_\alpha \cdot \vec{u}}{s^2} + \frac{9}{2} \frac{(\vec{e}_\alpha \cdot \vec{u})^2}{c^4} - \frac{3}{2} \frac{\vec{u} \cdot \vec{u}}{c^2}\right), \quad (28) \quad g_\alpha^{eq}(\vec{x}, t) = \epsilon \rho w_\alpha \left(1 + 3 \frac{\vec{e}_\alpha \cdot \vec{u}}{s^2} + \frac{9}{2} \frac{(\vec{e}_\alpha \cdot \vec{u})^2}{c^4} - \frac{3}{2} \frac{\vec{u} \cdot \vec{u}}{c^2}\right) \quad (29)$$

Here ρ , ϵ and \vec{u} are the macroscopic density, internal energy and velocity given by:

$$\rho = \sum_{i=0}^8 f_i, \quad (30) \quad \rho \vec{u} = \sum_{i=0}^8 f_i \vec{e}_i \quad (31) \quad \rho \epsilon = \sum_{i=0}^8 g_i. \quad (32)$$

The forcing terms F_i and G_i are problem dependent. For thermal convection $G_i = 0$ and F_i is a gravitational term Δf_α :

$$\Delta f_\alpha = -w_\alpha \rho \alpha \epsilon \frac{\vec{e}_\alpha}{|\vec{e}_\alpha|} \cdot \vec{g} \frac{1}{\tau_{grav}}, \quad (33)$$

where $||$ is the vector norm and \vec{g} is the gravitational acceleration. Here τ_{grav} is the relaxation time for the gravitational field. We take $\tau_g = 0.6$ here, following [3]. The algorithm used to evolve the above TLBM equations is given in algorithm 1

Algorithm 1 Thermal Lattice Boltzman Algorithm

```

 $f_\alpha = \rho_0 w_\alpha$ 
 $\epsilon = 0$ 
 $\epsilon_b$ 
 $\rho = 0$ 
 $\vec{u} = 0$ 
while Simulation Running do
     $g_\alpha = \rho \epsilon_b w_\alpha$ 
    if  $x - \vec{e}_\alpha$  is solid then
         $f_\alpha(x) = f_{\alpha'}(x)$ 
         $g_\alpha(x) = g_{\alpha'}(x)$ 
    else
         $f_\alpha(x) = f_\alpha(x - \vec{e}_\alpha)$ 
         $g_\alpha(x) = g_\alpha(x - \vec{e}_\alpha)$ 
    end if
     $\rho = \sum_{i=0}^8 f_i$ 
     $\vec{u} = \frac{(\sum_{i=0}^8 f_i \vec{e}_i)}{\rho}$ 
     $\epsilon = \frac{\sum_{i=0}^8 g_i}{\rho}$ 
     $f_\alpha^{eq} = \rho w_\alpha \left(1 + 3 \frac{\vec{e}_\alpha \cdot \vec{u}}{s^2} + \frac{9}{2} \frac{(\vec{e}_\alpha \cdot \vec{u})^2}{c^4} - \frac{3}{2} \frac{\vec{u} \cdot \vec{u}}{c^2}\right)$ 
     $g_\alpha^{eq}(\vec{x}, t) = \epsilon \rho w_\alpha \left(1 + 3 \frac{\vec{e}_\alpha \cdot \vec{u}}{s^2} + \frac{9}{2} \frac{(\vec{e}_\alpha \cdot \vec{u})^2}{c^4} - \frac{3}{2} \frac{\vec{u} \cdot \vec{u}}{c^2}\right)$ 
     $\Delta f_\alpha = -w_\alpha \rho \alpha \epsilon \frac{\vec{e}_\alpha}{|\vec{e}_\alpha|} \cdot \vec{g}$ 
     $\tau_g = \frac{3\kappa}{S^2\Delta t} + \frac{1}{2}$ 
     $\tau_f = \frac{3\nu}{S^2\Delta t} + \frac{1}{2}$ 
     $f_\alpha = f_\alpha + \frac{f_\alpha^{eq} - f_\alpha}{\tau_f} + \Delta f_\alpha$ 
     $g_\alpha = g_\alpha + \frac{g_\alpha^{eq} - g_\alpha}{\tau_g}$ 
end while

```

Boundary Conditions

In both streamfunction-vorticity codes, boundaries are set to be fluid-impermeable, non-slip and insulating. In the Lattice Boltzman code, "bounce back" boundary condition was used. This is a fluid-impermeable, insulating and slip boundary.

Advection tests

Here I present some simple tests that show how accurately my advection scheme is performing in both geometries. Next we tested the accuracy of the advection schemes. Thermal diffusivity (κ) and thermal expansion (α) were set to zero to avoid convection. The fluid was set to temperature 0 (arb. units) except a small segment which was set to 1 shown in yellow top left of figure 2, 3, 4, 5. A streamfunction ψ_c was enforced to produce diagonal back and forth motion or a continuous horizontal or azimuthal motion to cross a periodic boundary. Details of the streamfunctions used are given in appendix.

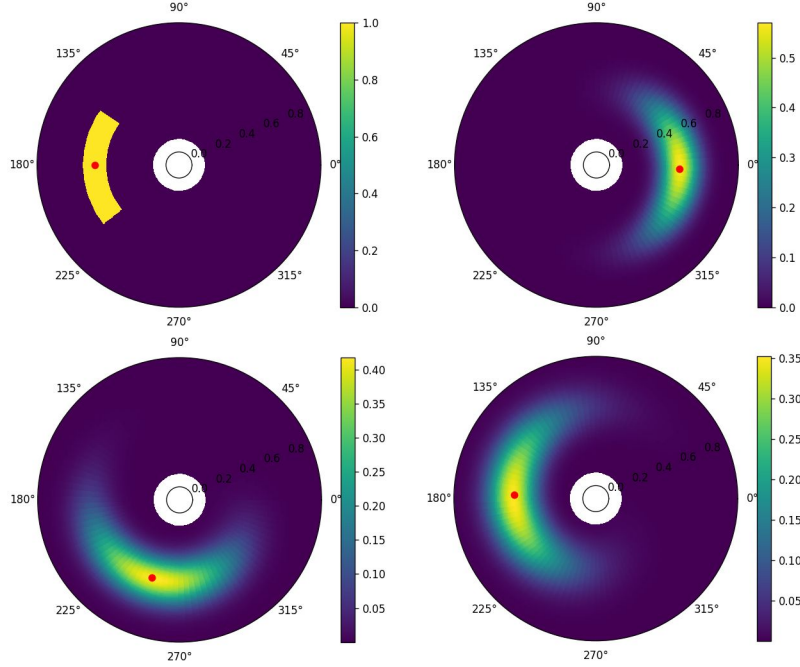


Figure 2: Polar azimuthal advection test. Temperature (color) is plotted in polar space. Red dot indicates temperature weighted mean position within the fluid and is taken as the location of the temperature 1 zone. Fluid is advected by an anticlockwise flow. Chronological order is Top left, top right, bottom left, bottom right. Top left shows the initial condition. Top right shows advection across periodic boundary. Bottom left is state when an exact scheme would have returned to the original position. Bottom right is the final state after being advected around one rotation.

The advection results for both codes are similar. For the periodic advection test figures 2 and 4 the temperature 1 region was advected across the periodic boundary without additional distortion. The centroid (red dot) also lagged the advection field by $\approx 1\%$ and $\approx 10\%$ for the cartesian (figure 4) and polar case (figure 2) respectively. It is unknown why these differ substantially, but a probable cause is a smaller timestep used to produce the polar tests. In all cases, the blurring shows numerical diffusion which happens along the direction of the advection field as predicted by equation ???. The discontinuity in temperature in figure 3 (bottom left) near the azimuthal 0 to 360 boundary is a result of setting a streamfunction with a discontinuity here.

Simulations

The cartesian and polar streamfunction-vorticity codes are limited in two distinct ways. The polar geometry of the 2-dimensional inner core is well suited to polar coordinates. However, by using polar coordinates, a singularity in the governing equations occurs at the center $r \rightarrow 0$. For standard regularly spaced meshes as is used here, this causes the lattice spacing near the center to become infinitesimal requiring small timesteps and large amounts of compute time. For this reason, the inner region of the polar domain is excluded leaving out a critical region in the simulation. In cartesian coordinates, there is no singularity and the full domain is included, however it becomes difficult to recreate the polar geometry and enforce boundary conditions. Because of this, we approximate the 2-dimensional inner core by "unrolling" as shown in figure 6, losing the affect of the polar geometry.

How much does the geometry matter

In this section I compare the results from the polar and cartesian streamfunction-vorticity codes with similar Prandtl and Rayleigh number to see how the geometry affects convection.

A gravitational field linearly proportional to height and radius for the cartesian and polar codes respectively was set. A constant internal heating field H was set for all but the upper 10% of both domains. A compensating heating field was set at the remaining top of the domain to balance the total heat generation. Note this heat field is different in the cartesian and polar cases. In all heating fields time-independent random fluctuations of $\approx 1\%$ were set to facilitate instabilities.

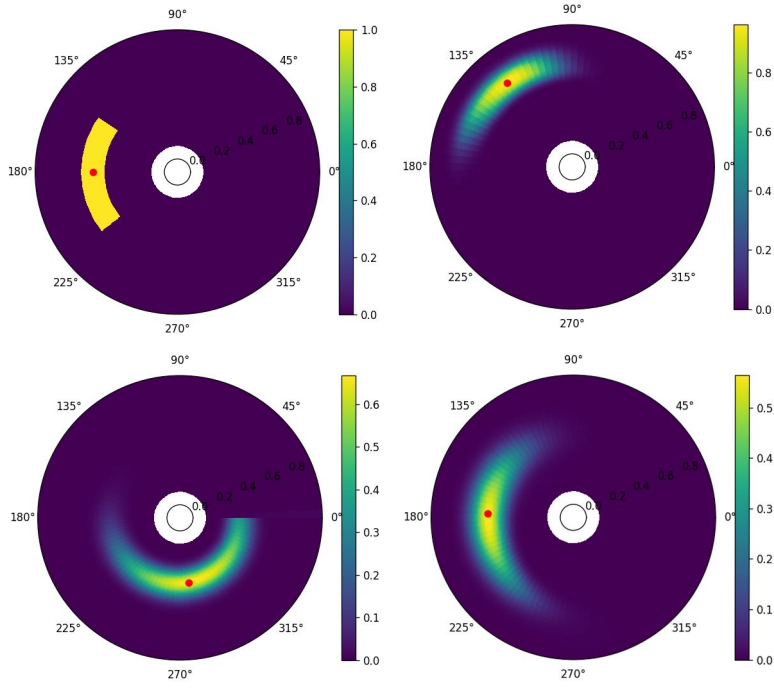


Figure 3: Polar coordinate diagonal advection test. Similar convection used to figure 2. Fluid is diagonally advected over a time t from the initial state (top left) to top right. The advection field is reversed for time $2t$ giving bottom left. The field is reversed again producing bottom right.

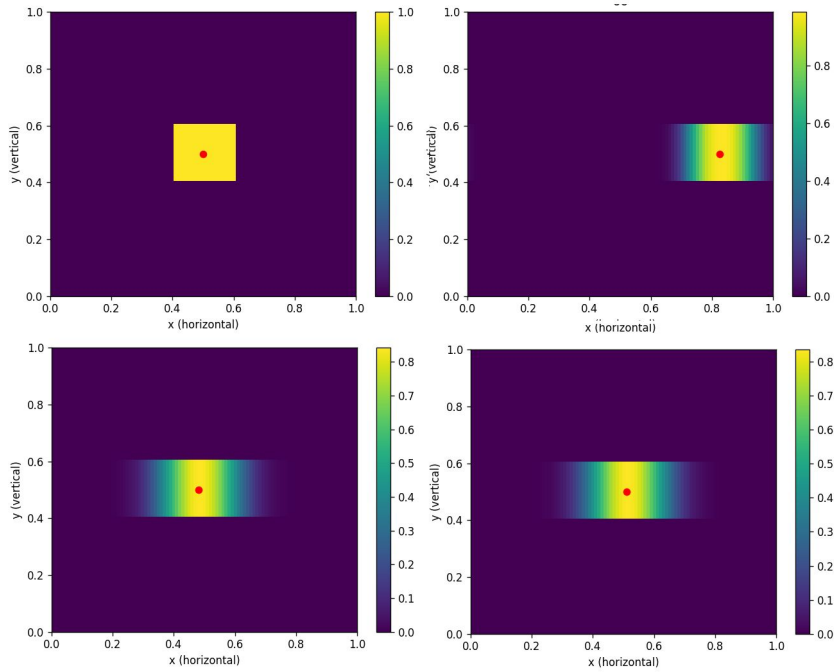


Figure 4: Cartesian coordinate advection test across a periodic boundary. Convention similar to figure 2.

As seen in figure 7, the two geometries give vastly different convective behaviour. The cartesian geometry (left) begins forming convective plumes at time ≈ 143000 , long after the time 25000 when the polar (right) model begins to convect. The convection patterns formed in the cartesian model are constant in time, forming the typical convection cells. The polar case is much more erratic, not forming typical convection cells. Finally, the wavelength for convection patterns in the cartesian case is approximately $1/5$ that produced by the polar case. In general, the polar case shows more vigorous convection characteristic of a higher effective rayleigh number.

Does the inner circle matter?

Here I keep the polar geometry and change the size of the central region to test its importance to the solution

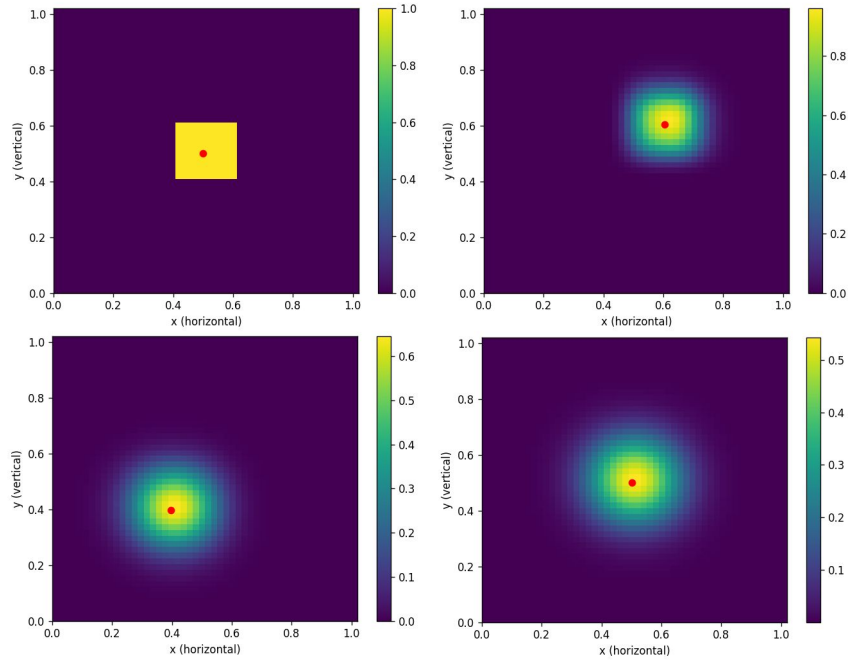


Figure 5: Cartesian diagonal advection test. Similar convention to figure 3.



shutterstock.com · 1188115291

Figure 6: figure showing how the 2-dimensional polar domain is "unrolled" into a 2-dimensional cartesian domain.

Thermal Lattice Boltzman Simulations

We have seen from the streamfunction-vorticity codes that geometry and internal region alter convection significantly, however, neither streamfunction-vorticity code can incorporate both.

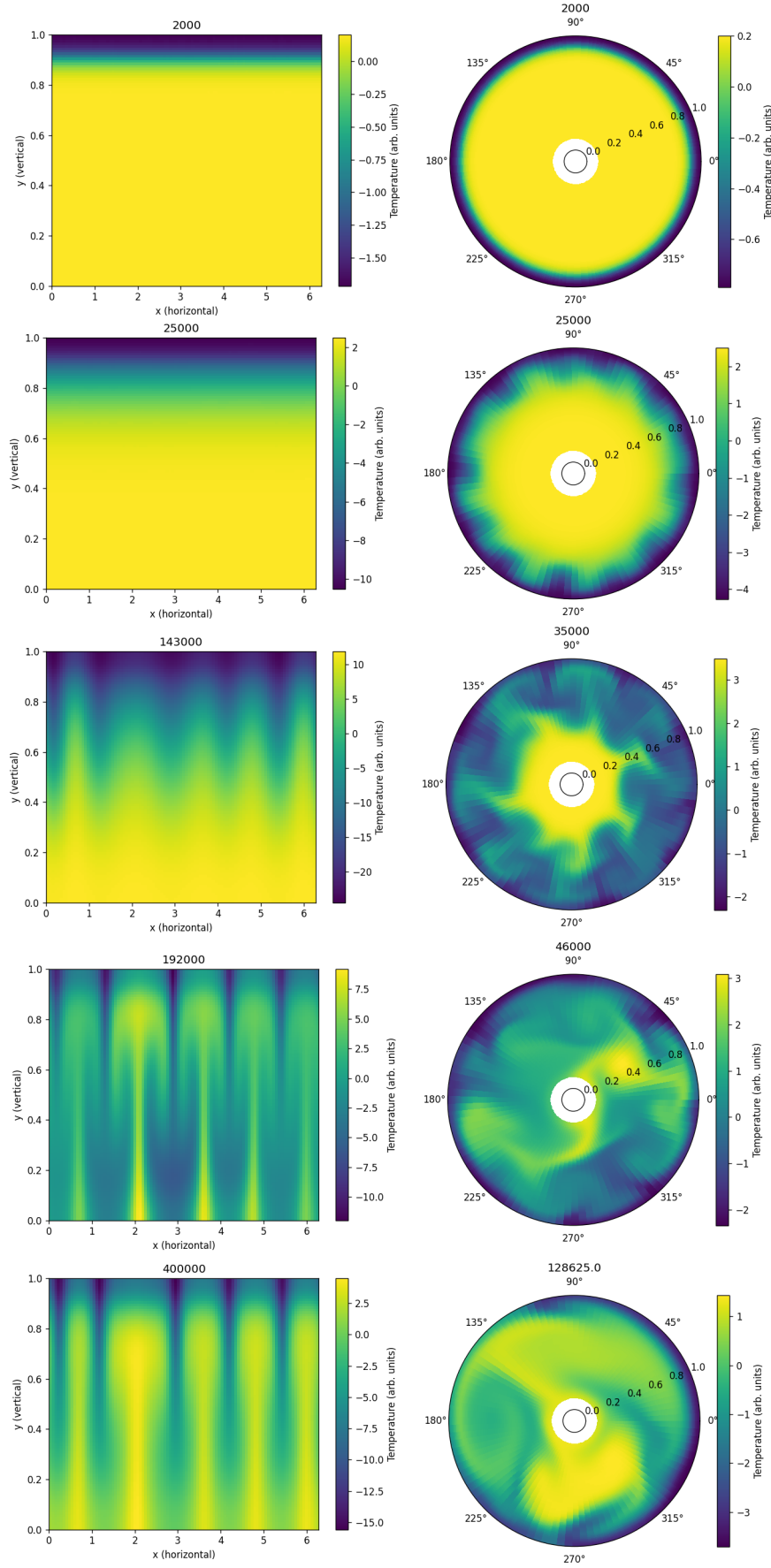


Figure 7: Internally Heated Convection comparison between cartesian case (left) and polar case (right) $Pr = 1, Ra = 10^8$. Times are given as headings. All other computation parameter settings are equivalent.

Dicussion

Conclusion

Appendix

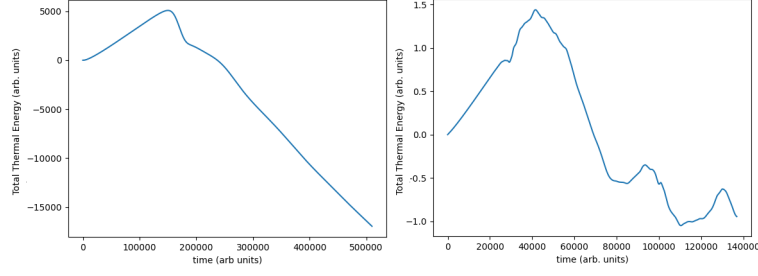


Figure 8: Total heat energy in cartesian (left) and polar (right) simulation through time in figure 7

Some Scales that I used

This is an important source here [1].

We chose the following length scales for the problem. For length we used d , the height or radius of the domain, for timescale we used $\frac{d^2}{\kappa}$, for pressure we used $\frac{\rho_0 d^2}{\kappa}$, for temperature we used $\frac{d^2 H}{\kappa}$. I took the rayleigh number as $Ra = \frac{g \alpha H d^5}{\nu \kappa^2}$ and the Prantl number $Pr = \frac{\nu}{\kappa}$. I additionally define a timescale for transport via flow:

$$\tau = \frac{\kappa \mathcal{V}}{g \alpha H d^3} \quad (34)$$

References

- [1] D. Goluskin. *Internally heated convection and Rayleigh-Bénard convection*. Springer, 2016.
- [2] R. Khazaeli, M. Ashrafizaadeh, and S. Mortazavi. A ghost fluid approach for thermal lattice boltzmann method in dealing with heat flux boundary condition in thermal problems with complex geometries. 2015.
- [3] P. Mora and D. A. Yuen. Simulation of plume dynamics by the lattice boltzmann method. *Geophysical Journal International*, 210(3):1932–1937, 2017.